



Universiteit
Leiden
The Netherlands

Mesenchymal stem cells in skeletal muscle regeneration

Garza-Rodea, A.S. de la

Citation

Garza-Rodea, A. S. de la. (2011, September 28). *Mesenchymal stem cells in skeletal muscle regeneration*. Retrieved from <https://hdl.handle.net/1887/17877>

Version: Corrected Publisher's Version

License: [Licence agreement concerning inclusion of doctoral thesis in the Institutional Repository of the University of Leiden](#)

Downloaded from: <https://hdl.handle.net/1887/17877>

Note: To cite this publication please use the final published version (if applicable).

Chapter 7

Exploitation of herpesvirus immune evasion strategies to generate non-immunogenic human mesenchymal stem cells for use in regenerative medicine

AS de la Garza-Rodea, MC Verweij, H Boersma, I van der Velde-van Dijke, AA de Vries, RC Hoeben, DW van Bekkum, EJ Wiertz, S Knaän-Shanzer
PLoS One. 2011;6:e14493.

Abstract

Background

Mesenchymal stem cells (MSCs) are multipotent cells residing in the connective tissue of many organs and holding great potential for tissue repair. In culture, human MSCs (hMSCs) are capable of extensive proliferation without showing chromosomal aberrations. Large numbers of hMSCs can thus be acquired from small samples of easily obtainable tissues like fat and bone marrow. MSCs can contribute to regeneration indirectly by secretion of cytokines or directly by differentiation into specialized cell types. The latter mechanism requires their long-term acceptance by the recipient. Although MSCs do not elicit immune responses *in vitro*, animal studies have revealed that allogeneic and xenogeneic MSCs are rejected.

Methodology/Principal Findings

We aim to overcome MSC immune rejection through permanent down-regulation of major histocompatibility complex (MHC) class I proteins on the surface of these MHC class II-negative cells through the use of viral immune evasion proteins. Transduction of hMSCs with a retroviral vector encoding the human cytomegalovirus US11 protein resulted in strong inhibition of MHC class I surface expression. When transplanted into immunocompetent mice, persistence of the *US11*-expressing and HLA-ABC-negative hMSCs at levels resembling those found in immunodeficient (i.e. NOD/SCID) mice could be attained provided that recipients' natural killer (NK) cells were depleted prior to cell transplantation.

Conclusions/Significance

Our findings demonstrate the potential utility of herpesviral immunoevasins to prevent rejection of xenogeneic MSCs. The observation that down-regulation of MHC class I surface protein expression renders hMSCs vulnerable to NK cell recognition and cytolysis implies that multiple viral immune evasion proteins are likely required to make hMSCs non-immunogenic and thereby universally transplantable.

Introduction

Mesenchymal stem cells (MSCs) are multipotent cells present in the stroma of most organs. Their isolation relies on adherence to cell culture plastics. In culture, human MSCs (hMSCs) are capable of extensive proliferation without giving rise to chromosomal aberrations¹. Large numbers of hMSCs can thus be obtained from small samples of easily accessible tissues like fat and bone marrow (BM).

MSCs are identified primarily on the basis of their ability to differentiate under specific culture conditions into various mesodermal cell types, including osteoblasts, chondrocytes and adipocytes. Since markers exclusively displayed on the surface of MSCs have not been identified yet, these cells are phenotypically characterized by a combination of several non-hematopoietic cell surface markers².

Typically, cultured hMSCs express on their surface the major histocompatibility complex (MHC) class I human leukocyte antigens A, B, C (HLA-ABC) and HLA-G, but not HLA-E^{3,4} and our unpublished observations. Furthermore, hMSCs do not display MHC class II (HLA-DR) proteins on their plasma membrane. MHC class II molecules are present, however, in intracellular reservoirs and can be recruited to the cell surface through exposure to interferon gamma (IFN- γ)^{5,6}.

Recently, cultured MSCs were shown to have pleiotropic immunomodulatory properties *in vitro* including suppression of T cell proliferation in response to alloantigens or mitogens^{7,8}, inhibition of B cell proliferation and antibody production^{9,10} and inhibition of dendritic cell maturation^{11,12}. Also, cultured hMSCs are not lysed by freshly isolated allogeneic natural killer (NK) cells but are susceptible to the lytic activity of activated NK cells^{13,14}. *In vivo*, allogeneic MSCs were shown to prolong the survival of skin allografts in baboons⁷ and hMSCs ameliorated experimental autoimmune encephalitis in mice¹⁵. In patients, infusion of allogeneic hMSCs has been shown to mitigate acute graft-versus-host disease to various degrees¹⁶⁻¹⁸. The reputation “non-immunogenic” that has been bestowed upon MSCs on the basis of these findings, has been challenged by studies with laboratory animals showing rejection of MSCs in allogeneic transplantation settings. The therapeutic benefits that have been observed after *in vivo* administration of MSCs are thus commonly believed to result mainly or exclusively from paracrine effects¹⁹.

Repair of tissue damage that requires *in situ* differentiation of MSCs into specialized cell types or their fusion with resident cells has been attained only with autologous/syngeneic MSCs or in immunocompromised recipients²⁰⁻²⁵. Similarly, successful use of MSCs as vehicles for the delivery of therapeutics depends on immunocompatible donor–recipient combinations^{26,27}.

The involvement of surface-displayed MHC class I molecules in graft rejection and the mitigation of transplant immunogenicity through interference with MHC

class I protein recognition have been well documented. Masking of MHC class I molecules by specific antibodies enabled transplantation of human pancreatic islands and liver cells in mice and of porcine neurons in rats^{28,29}. Moreover, neurons of MHC class I transgenic mice were not rejected in rats³⁰. Along the same line, adipose tissue-derived hMSCs that had lost MHC class I surface expression during long-term culture, effectively contributed to skeletal muscle repair in immunocompetent dystrophic mice³¹. Recently, Zdoroveac and co-workers³² demonstrated reduced immune responses to carotid allografts genetically modified to decrease surface levels of MHC class I antigens through an endoplasmic reticulum targeted MHC class I-specific intrabody.

Inhibition of MHC class I surface expression is a mechanism evolved by viruses to prevent killing of their targets cells by the hosts' immune system^{33,34}. Examples are herpesviruses that encode so-called immune evasion proteins (also known as immunoevasins), which specifically target different steps of the MHC class I-mediated peptide presentation pathway to elude the activity of CD8⁺ T cells. Some of these proteins, like the bovine herpesvirus type 1 (BHV-1) UL49.5 protein and the Epstein-Barr virus (EBV) BNLF2a protein, are inhibitors of the transporter associated with antigen processing (TAP), an essential component of the MHC class I antigen presentation pathway³⁵⁻³⁷. Other herpesviral proteins like the human cytomegalovirus (HCMV) *US2* and *US11* gene products, target MHC class I molecules for destruction through dislocation of newly synthesized proteins into to the cytosol where they are degraded by proteasomes³⁸⁻³⁹. Herpesviruses also evolved strategies to interfere with the presentation of viral antigens to MHC class II-restricted CD4⁺ T cells and to escape NK cell responses⁴⁰⁻⁴¹.

In this study, we investigated whether immune rejection of foreign cells could be prevented by controlled permanent down-regulation of MHC class I surface expression. Using retroviral vectors (RVs) encoding four different herpesviral immunoevasins, we identified the *US11* protein as a very effective inhibitor of MHC class I surface display in hMSCs. The immunogenicity of MHC class I hMSCs should ideally have been tested in an allogeneic recipient. This not being feasible, we resorted to the use of mouse models to study the *in vivo* persistence of hMSCs displaying normal or greatly reduced numbers of MHC class I molecules at their plasma membrane. In this xenotransplantation setting, we found *US11*-transduced hMSCs to be protected from rejection in immunocompetent recipients, albeit only after depletion of NK cells. This is, to our knowledge, the first *in vivo* study demonstrating the utility of herpesviral immunoevasins to modulate the immunogenicity of transplanted culture-expanded primary human cells.

Materials and methods

Isolation and culture of BM-derived hMSCs

hMSCs were obtained from BM samples of four donors (2 males and 2 females; age range 38 to 72 years) collected during orthopedic surgery with a written informed consent and according to the guidelines of the Leiden University Medical Center (LUMC, Leiden, the Netherlands). hMSCs were isolated from the BM samples as described previously³. Briefly, the cells were seeded in Dulbecco's modified Eagle's medium (DMEM; Invitrogen-Gibco, Breda, the Netherlands) containing 100 U/ml penicillin (Invitrogen-Gibco), 100 µg/ml streptomycin (Invitrogen-Gibco) and 10% fetal bovine serum (FBS; Invitrogen-Gibco) in plastic cell culture flasks (Greiner Bio-One, Alphen aan den Rijn, the Netherlands) and incubated for 48 hours at 37°C in humidified air and 10% CO₂. Thereafter, the non-attached cells were removed and the adherent cells were grown to 70% confluency before transfer for further expansion³. At passage number 2, aliquots of 2×10^5 cells were cryopreserved. hMSC expansion was performed in culture medium supplemented with 0.5 ng/ml basic fibroblast growth factor (Sigma-Aldrich, St. Louis, MO). Cell replication was monitored for up to 15 passages from cultures initiated by seeding 5×10^4 /cm² of freshly thawed cells in 25-cm² cell culture flasks (Greiner bio-One, Frickenhausen, Germany). After reaching 70-80% confluency, the total number of cells in each culture was determined and a fraction of them was re-plated for a next passage under the same conditions as before.

The characterization of the cultured hMSCs by immunophenotyping and *in vitro* differentiation assays has been reported before^{3,66}.

Viral vectors and hMSC transduction

The coding sequences of the BHV-1 *UL49.5*, EBV *BNLF2a* and HCMV *US2* and *US11* genes were amplified from viral DNA by polymerase chain reaction (PCR). The resulting PCR fragments were inserted in the gammaretroviral vector shuttle plasmid pLZRS-IRES-GFP upstream of the internal ribosome entry site as described previously^{35,36,67,68}. Recombinant retroviruses directing the synthesis of eGFP and either of the four herpesviral immunoevasins were prepared using the Phoenix amphotropic packaging system as described previously⁶⁹.

Culture-expanded hMSCs (passages 4 to 8) were transduced with the recombinant retroviruses in RetroNectin (Takara Bio Europe, Saint-Germain-en-Laye, France)-coated dishes. Two or three rounds of transduction were performed at 24-hour intervals.

For *in vivo* studies, RV-transduced hMSCs were sorted on the basis of eGFP levels using a FACSDiva (Becton Dickinson [BD], Breda, the Netherlands). The

eGFP⁺ MHC class I⁻ cells as well as untransduced hMSCs from the same batch of cells were then exposed to the vesicular stomatitis virus G protein-pseudotyped self-inactivating lentiviral vector LV.C-EF1a.cyt-bGal⁷⁰, encoding *Escherichia coli* β -gal. The cells were incubated for 4 hours with 2 HeLa cell-transducing units of the LV.C-EF1a.cyt-bGal vector/hMSC in DMEM containing 10% FBS and 8 μ g/ml hexadimethrine bromide (polybrene; Sigma-Aldrich) at 37°C⁷¹. Transduction efficiencies were determined 14 days later by staining the cells with 2 mM 5-bromo-4-chloro-3-indolyl- β -D-galactopyranoside (Sigma-Aldrich) as described previously⁷². Typically, more than 90% of the LV.C-EF1a.cyt-bGal-transduced hMSCs were β -gal⁺ at this time point as well as after multiple *ex vivo* cell doublings.

Antibodies and flow cytometry

Flow cytometric analyses were performed with a FACSort (BD) using the following murine monoclonal antibodies (MAbs): phycoerythrin (PE)-conjugated anti-human CD44 (clone G44-26; BD), PE-conjugated anti-HLA-ABC complex (clone W6/32; Dako Netherlands, Heverlee, Belgium) and PE-conjugated anti-HLA-DR (clone L243; BD). NK cells in the peripheral blood samples of the recipient mice were detected with PE-conjugated anti-mouse NK1.1 (clone PK126; BD), fluorescein isothiocyanate (FITC)-conjugated anti-mouse CD3 (clone 17A2; BD) and peridinin-chlorophyll-protein-complex (PerCP)-conjugated anti-mouse CD45 (clone 30-F11; BD) MAbs. Control MAbs (mouse IgGs conjugated with FITC, PE or PerCP; BD) were used for gate positioning.

Immunoblotting

RV-transduced hMSCs were lysed in 0.5% Nonidet P-40, 50 mM Tris-HCl (pH 7.5), 5 mM MgCl₂, 10 μ M leupeptin (Sigma-Aldrich) and 1 mM 4-(2-aminoethyl) benzenesulfonyl fluoride (Sigma-Aldrich). The proteins in the lysates were separated by sodium dodecyl sulfate-polyacrylamide gel electrophoresis and transferred to polyvinylidene fluoride membranes (Hybond-P; GE Healthcare Europe, Diegem, Belgium). The resulting blots were incubated with the rat monoclonal antibody MVH 5B9 for the detection of BNLFA2a⁷³, a rabbit polyclonal antiserum directed against amino acids 22 through 51 of the BHV-1 UL49.5 protein⁷⁴ or a rabbit polyclonal antiserum specific for the N-terminus of the HCMV US2 protein (amino acids 24 through 41;⁶⁸). For the detection of the HCMV US11 protein, a rabbit antiserum directed against the N-terminus of the protein was used (amino acids 21 through 38;⁶⁷). Horseradish peroxidase-conjugated secondary antibodies (Dako Netherlands) and Amersham ECL Plus Western Blotting Detection Reagents (GE Healthcare Europe) were used to visualize bound primary antibodies.

Mice and the xenotransplantation model

NOD/LtSz-scid/scid/J (NOD/SCID) mice were bred in the animal facilities of the LUMC from breeding pairs purchased from Jackson Laboratories (Bar Harbor, ME). Animals were housed under specific pathogen-free conditions as described previously⁷⁵.

C57Bl/6J (H-2^b) (C57Bl) mice were purchased from Harlan (Venray, the Netherlands). Male and female mice 8-12 weeks old were used. The animal room was on a 12:12 hours light-dark cycle and kept at 22°C. Standard laboratory chow and sterile water were provided ad libitum. All experiments were performed according to a study protocol approved by the Animal Ethics Committee of the LUMC.

hMSC engraftment was studied by subcutaneous injection of $3\text{-}5 \times 10^5$ *LacZ*-tagged cells in a total volume of 20 μl phosphate-buffered saline (PBS) into the pinna of one of the ears of either NOD/SCID mice, C57Bl mice or C57Bl mice that had been depleted of NK cells by intraperitoneal injection of 100 μg per treatment of sodium azide-free affinity purified anti-mouse NK1.1 MAbs (clone PK136; BD or BioLegend, San Diego, CA). Antibody administration was initiated 24 hours prior to hMSC implantation and repeated once a week thereafter. The level of NK cells in these mice was determined by flow cytometric analysis of PBMCs that were sampled prior to each antibody injection and before sacrificing the mice. PBMCs of untreated mice served to derive control values.

The relative amount of *LacZ*-expressing human cells in the ears of the treated mice was determined with the Beta-Glo assay system (Promega Corporation, Madison, WI)^{76,77}. At different time points after hMSC implantation, mice were sacrificed, the whole treated ear was dissected, snap-frozen in liquid nitrogen and stored at -80°C until processing. Each ear was homogenized in 1 ml of homogenization buffer (10 mM KCl, 1.5 mM MgCl₂ and 10 mM Tris-HCl [pH 7.4]) on ice as described⁷⁸. The homogenate was cleared by centrifugation for 10 minutes at $20,800 \times G$ and 4°C. The supernatants were analyzed for β -gal activity according to the protocol provided by the manufacturer of the Beta-Glo assay system. Chemoluminescence was measured using a Wallace 1420 VICTOR 3 multilabel plate reader (PerkinElmer Nederland, Groningen, the Netherlands). β -gal activity was expressed in RLU. Serial dilutions of each supernatant were analyzed and plotted against RLU. RLU of different samples were compared at a dilution positioned in the linear range of the dose-response curve.

For each experimental group, the β -gal activity at each time point is presented as a percentage of the average β -gal activity detected in the ears of mice immediately (i.e. within 5 minutes) after cell injection (time 0; 100%), allowing a direct comparison of all experimental groups in the four *in vivo* experiments that were performed.

Immunohistology of pinna

C57Bl mice were injected as above with *LacZ*-tagged hMSCs. Three mice per treated group were sacrificed at 3, 7 and 14 days after cell injection. Ears were dissected and frozen by liquid nitrogen for one minute and stored at -80°C until further processing. Three consecutive transversal cross-sections of $8\ \mu\text{m}$ were placed on SuperFrost Plus glass slides (Menzel-Gläser, Braunschweig, Germany) and stored at -20°C .

The first slide of each pinna was processed for X-gal staining as described before⁷⁰. Sections were counterstained with nuclear fast red and saffron according to standard procedures and mounted in Entellan mounting medium (Merck, Schiphol-Rijk, the Netherlands).

Immunostaining of the tissues was performed with antibodies specific for CD8 and NK cells. The sections were fixed with ice-cold acetone (Mallinckrodt Baker, Deventer, the Netherlands) for 5 minutes at 4°C , air-dried and washed once for 5 minutes with PBS. A peroxidase blocking step was performed by incubating the sections for 10 minutes with 0.3% H_2O_2 in H_2O followed by two PBS washes for 5 minutes each. Sections were then treated with the M.O.M. Immunodetection Kit Basic (Vector Laboratories, Burlington, CA) accordingly to the manufacturer's specifications. For the staining of CD8^+ cells, biotinylated rat anti-mouse CD8a MAb (Biolegend; clone 53-6.7; IgG2a; 1:250) was added for overnight incubation at 4°C . As isotype control antibody we used biotin-conjugated rat IgG2a MAb (Biolegend; clone RTK2758; 1:200). Antibodies were removed by washing twice with PBS for 5 minutes. The Vectastain Elite ABC Kit (Vector Laboratories) was then applied according to manufacturer's specifications. Bound antibody complexes were visualized with 3,3'-diaminobenzidine (DAB, Sigma-Aldrich). Sections treated with DAB only were used to stain granulocytes. Finally, the sections were counter-stained with hematoxylin, dehydrated and mounted in Entellan mounting medium. Images were captured with a ColorView Illu camera (Olympus Nederland, Zouterwoude, the Netherlands) mounted on a Leitz Wetzlar Diaplan microscope (Germany) and processed with Cell^B imaging software (Olympus).

Three antibodies were used for the detection of NK cells: the biotinylated mouse anti-mouse NK1.1 MAb (Biolegend; clone PK136; IgG2a; 1:10), the goat anti-mouse Nkp46 polyclonal antibody (R&D Systems Europe, Abingdon, United Kingdom; IgG; 1:100) and the rat anti-mouse Ly49G2 MAb (BD; clone 4D11; IgG2a; 1:20). The corresponding isotype controls were a mouse IgG2a MAb (Biolegend; clone MOPC-173; 1:200), goat serum (1:10) and the previously mentioned biotin-conjugated rat IgG2a MAb (1:200). Tissues were incubated overnight at 4°C with the first antibody. After washing with PBS, tissues were exposed to a 2.5-hour incubation with streptavidine-conjugated Qdot 655 (Invitrogen-Molecular Probes; 1:200), Alexa 594-coupled donkey

anti-goat IgG (Invitrogen-Molecular Probes; 1:800) or Alexa 488-conjugated donkey anti-rat IgG (Invitrogen-Molecular Probes; 1:400), respectively. PBS-washed sections were then incubated with Hoechst 33342 (1:1000 in PBS, Invitrogen-Molecular Probes) for 10 minutes, washed thoroughly (3-4 times) with PBS and mounted in Vectashield. Microscopic analysis was performed on using Leica DM5500 B fluorescence microscope (Leica Microsystems, Rijswijk, the Netherlands). Images were captured with a cool SNAP K4 CCD camera (Photometrics, Tucson, AZ) and archived with home-made software.

Statistics

Data were analyzed with the one-way analysis of variance. Results are expressed as the mean \pm standard deviation (SD). A p -value <0.05 was considered significant.

Results

Herpesviral immune evasion proteins greatly differ in their ability to inhibit HLA-ABC expression on the surface of hMSCs

Four different herpesviral immunoevasins were tested for their ability to alter the expression of HLA-ABC on the surface of hMSCs. To this end, hMSCs from a single donor (i.e. donor 1) were stably transduced with bicistronic RVs coding for the enhanced green fluorescent protein (eGFP) and for the product of the BHV-1 *UL49.5* gene (RV-UL49.5-eGFP), the EBV *BNLF2a* gene (RV-BNLF2a-eGFP), the HCMV *US2* gene (RV-US2-eGFP) or the HCMV *US11* gene (RV-US11-eGFP). Untransduced hMSCs and cells transduced with an RV coding for eGFP only (RV-eGFP) served as negative controls. Flow cytometric analysis performed 5, 30 and 90 days after transduction revealed that a large proportion of the cells in each of the transduced samples expressed eGFP (Figure 7.1A). The HLA-ABC levels on the plasma membrane of the eGFP⁺ cells, as determined by staining with HLA-ABC-specific antibodies differed, however, depending on the herpesviral gene present. Whereas untransduced and RV-eGFP-transduced hMSCs expressed high levels of plasma membrane-bound MHC class I molecules, HLA-ABC molecules were barely detectable on the surface of cells transduced with RV-US11-eGFP. A comparison of the HLA-ABC signal intensities between the GFP⁺ and GFP⁻ (i.e. untransduced) cells in the RV-US11-eGFP treated sample (Figure 7.1B) showed that forced *US11* expression causes a 46-fold reduction in HLA-ABC surface levels (mean fluorescent activity [MFI] of 5 and 229, respectively). Down-regulation of plasma membrane-bound HLA-ABC molecules was also observed in hMSCs exposed to RV-US2-eGFP albeit to a lesser extent (with a MFI ratio of untransduced versus transduced cells of 5.2).

In hMSCs transduced with the RVs encoding the BNLF2a or UL49.5 protein, HLA-ABC surface expression was reduced only marginally (for both vectors the MFI ratios of untransduced versus transduced cells was 1.2).

The similar frequency of eGFP⁺ cells and the similar average intensity of the eGFP signal in the eGFP⁺ cells in all RV-treated samples suggest that hMSCs had been transduced with approximately equal efficiency by the different RVs. Western blot analysis of proteins extracted from hMSCs at 21 days after transduction confirmed the presence of the UL49.5, BNLF2a, US2 and US11 proteins (Figure 7.1C).

Transduction of hMSCs isolated from the BM of three additional donors (i.e. donors 2, 3 and 4) with RV-US2-eGFP or RV-US11-eGFP yielded very similar results as for donor 1 (data presented in Figure. 7.2A and 7.2C). All cells with down-modulated HLA-ABC surface expression were also eGFP⁺. Furthermore, transduction with the RVs did not affect plasma membrane levels of the CD44 protein, a marker of hMSCs (Figure 7.2B).

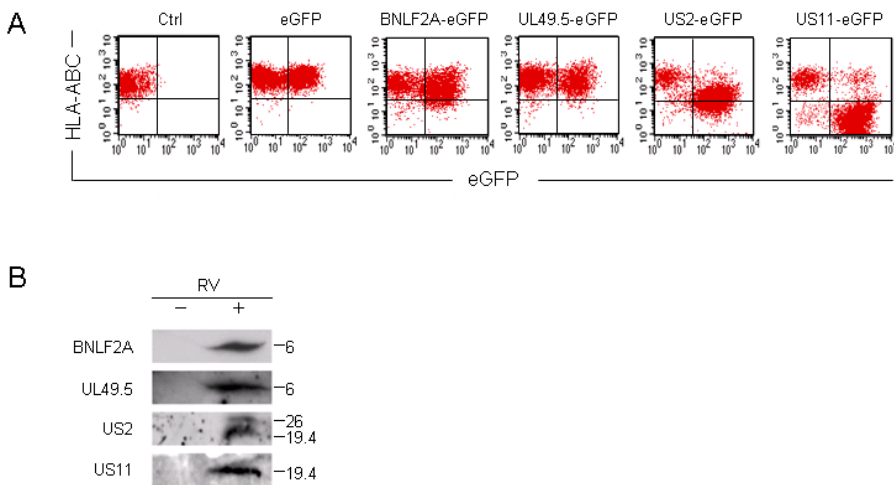


Figure 7.1 Different herpesviral immunoevasins inhibit MHC class I expression on hMSCs to a different extent. (A) Flow cytometric analysis of culture-expanded (Ctrl) hMSCs and of hMSCs transduced with RVs coding for eGFP alone or for eGFP and either the BHV-1 UL49.5, EBV BNLF2A, HCMV US2 or HCMV US11 protein. The data are from cells analyzed 30 days after transduction. Analysis of the hMSCs at 5 and 90 days post-transduction yielded very similar results (data not shown). MFIs of the HLA-ABC signal of eGFP⁻ (untransduced [UT]) and eGFP⁺ (transduced [T]) cell populations in each sample and their ratio are given below the dot plots **(B)**. **(C)** Western blot analysis of lysates from untransduced hMSCs (-) and of hMSCs transduced with RV-BNLF2A-eGFP, RV-UL49.5-eGFP, RV-US2-eGFP or RV-US11-eGFP (+). The specificity of the antibodies used is indicated at the left. Numbers at the right represent molecular weights in kilodalton (kDa). The 26-kDa and 19.4-kDa protein species recognized by the US2-specific antibodies correspond to N-glycosylated and non-glycosylated forms of the US2 protein, respectively.

Persistence of herpesviral immune evasion proteins in hMSCs does not compromise their replication capacity

hMSCs transduced to express either of the four herpesviral *immuno-evasion* genes were kept in culture for five additional passages. At each passage, the number of cells was determined and cell aliquots were analyzed for the presence of eGFP and surface HLA-ABC. Overall growth characteristics were not affected by the expression of the herpesviral *immuno-evasion* genes (Figure 7.3).

During the entire period of analysis, the frequency of eGFP⁺ cells, the average eGFP signal per eGFP⁺ cell, as well as the cell surface expression level of HLA-ABC remained constant (data not shown).

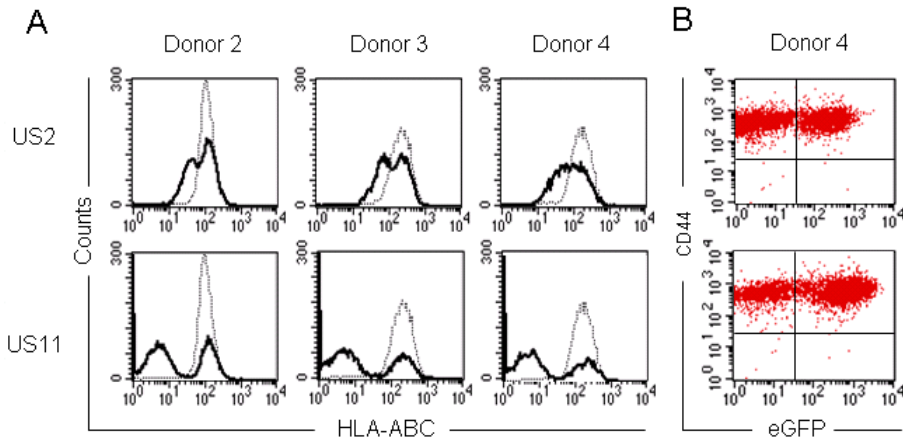


Figure 7.2 US2 and US11 inhibit MHC class I surface expression in hMSCs of different donors. (A) Flow cytometric analysis of HLA-ABC surface expression in hMSCs derived from the BM of three different donors. Gray lines represent untransduced hMSCs. Black lines correspond to hMSCs transduced with RV-US2-eGFP (upper panels) or with RV-US11-eGFP (lower panels). The presented data are from cells analyzed 30 days after transduction. (B) Flow cytometric analysis of CD44 surface expression in hMSCs of donor 4 at 30 days after transduction with RV-US2-eGFP (upper panel) or RV-US11-eGFP (lower panel). Similar results were obtained with cells of all other donors (data not shown). (C) Comparison of down-regulation of HLA-ABC surface expression by RV-US2-eGFP and RV-US11-eGFP. Shown are HLA-ABC MFI values of untransduced (gray bars) and transduced (black bars) cells of single samples of culture-expanded hMSCs from 4 donors (marked D1 to D4; values derived from data presented in Figure 7.1 and 7.2). The differences in the average MFI ratio (calculated as in Figure 7.1) between the hMSCs exposed to RV-US2-eGFP and those transduced with RV-US11-eGFP is highly significant (* $p=0.0005$).

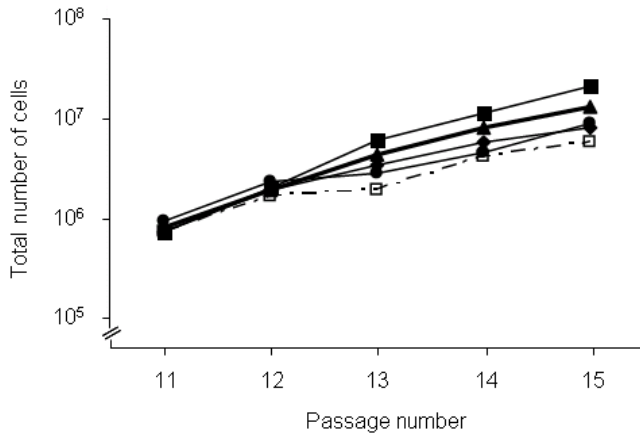


Figure 7.3 **Herpesviral immunoevasins do not compromise the replication rate of hMSCs in culture.** hMSCs were transduced at passage number 8 with bicistronic RVs encoding eGFP and a herpesviral immunoevasin and kept in culture for 7 additional passages. Lines represent untransduced hMSCs (□) and cells transduced with RV-UL49.5-eGFP (◆), RV-BNLF2A-eGFP (▲), RV-US2-eGFP (■) or RV-US11-eGFP (●) during 5 passages.

IFN- γ partially overrules US2- and US11-mediated down-regulation of MHC class I surface expression and elevates surface levels of MHC class II molecules

Previous studies have demonstrated that treatment of hMSCs with IFN- γ induces cell surface expression of MHC class II molecules^{5,6}. We confirmed this finding (Figure 7.4) with untransduced hMSCs and showed that the same applies to hMSCs transduced with RV-US2-eGFP or RV-US11-eGFP. In all three cell populations surface MHC class II levels were equally high after incubation for 48 hours with 100 ng/ml of IFN- γ . Surface MHC class I expression after IFN- γ treatment depended on the levels of plasma membrane-bound MHC class I molecules prior to cytokine stimulation, i.e. HLA-ABC surface expression in RV-US2-eGFP-transduced hMSCs was similar to that in untransduced cells not treated with IFN- γ but it was only partially restored in cells transduced with RV-US11-eGFP.

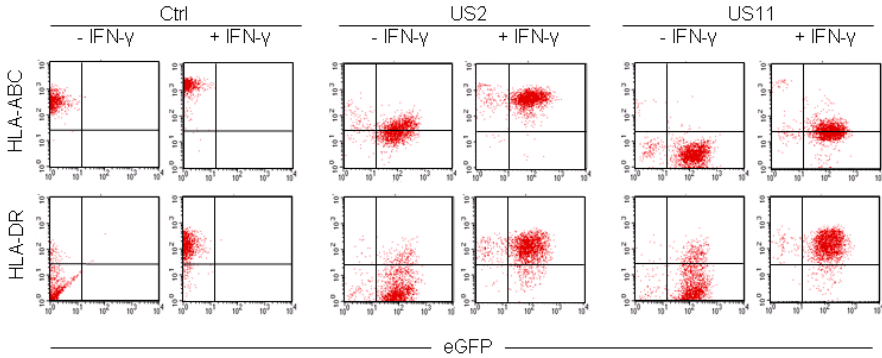


Figure 7.4 **IFN- γ modulates expression of MHC class I and class II molecules on US2- and US11-transduced hMSCs.** Flow cytometric analysis of the expression of MHC class I (HLA-ABC; upper panels) or MHC class II (HLA-DR; lower panels) proteins on the surface of untransduced hMSCs (Ctrl) and of cells transduced with RV-US2-eGFP (US2) or with RV-US11-eGFP (US11). The cells were (+ IFN- γ) or were not (- IFN- γ) incubated for 48 hours with 100 ng/ml IFN- γ prior to flow cytometry. The US11- and US2-transduced hMSCs used for this experiment, were sorted on the basis of eGFP expression.

Persistence of HLA-ABC-negative hMSCs in immunocompetent mice requires depletion of NK cells

The effect of MHC class I surface expression on the engraftment of hMSCs in mice was addressed by comparing the persistence of RV-US11-eGFP-transduced hMSCs (US11-hMSCs) with that of unmodified cells after intrapinnal implantation into immunodeficient or immunocompetent mice.

To allow quantification of the surviving donor cells, we used in this study US11-hMSCs and control hMSCs that were endowed with a recombinant *LacZ* gene by transduction with the self-inactivating lentiviral vector LV.C-EF1a.cyt-bGal. The β -galactosidase (β -gal) activity in treated ears was determined with the Beta-Glo assay system. Validation of this assay system revealed a linear correlation between β -gal activity (expressed in relative light units [RLUs]) and the number of donor cells injected (Figure 7.5A).

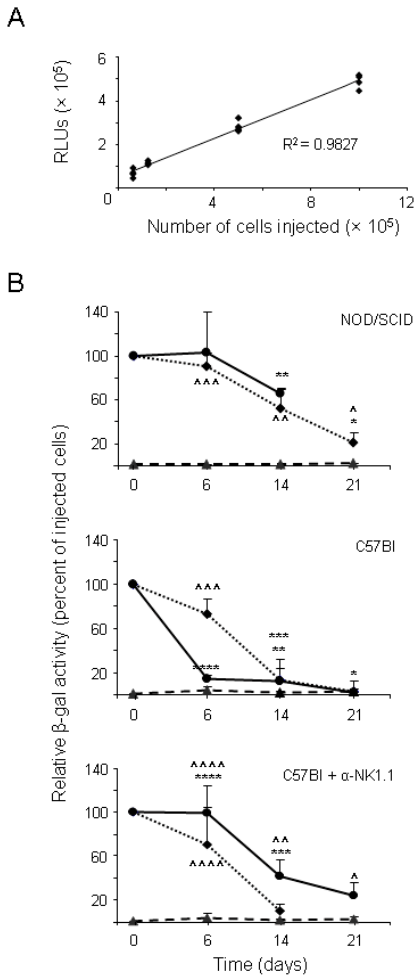


Figure 7.5 Engraftment of hMSCs with modulated surface MHC class I expression in immunodeficient and immunocompetent mice. (A) Correlation between donor cell number and β -gal activity (expressed in RLUs) in the ears of mice following intrapinnal injection of *LacZ*-expressing hMSCs. The ears of the treated mice (four mice for each cell dose) were excised 5 minutes after cell injection and processed as described in the Materials and Methods section. Each dot represents a single ear. (B) Engraftment of hMSCs in immunodeficient mice (upper graph), immunocompetent mice (middle graph) and immunocompetent mice depleted of NK cells (lower graph). Indicated on the vertical axis is the average β -gal activity in whole ears of mice sacrificed at the specified time points after the injection of cell or PBS as compared to that of mice killed 5 minutes after the injection of cells from the same batch (time 0; 100%). The graphs show time-related changes in relative β -gal activity for sorted US11-hMSCs (solid line and \bullet) and for untreated hMSCs (dotted line and \blacklozenge) in NOD/SCID mice, C57BI mice and NK cell-depleted C57BI mice. Background β -gal activity values were derived from mice whose pinnae were injected with vehicle only (broken line and \blacktriangle). Individual data points represent the average (\pm SD) relative β -gal activity of 3 to 14 animals and have been derived from 2 to 4 independent experiments. Statistical analysis was performed at each time point and through all three graphs for pairs of data points derived from all mice in a particular experimental group. Significant difference ($p < 0.002$) between data points were marked s1 and s2 while non-significant differences ($p > 0.5$) between data pairs are indicated by n1 and n2.

In the immunodeficient NOD/SCID mice, the survival of control (i.e. HLA-ABC⁺) hMSCs and US11-hMSCs was similar during the first 14 days after implantation with a reduction in β -gal activity to 52 ± 19 and $65\pm 4\%$ of day 0 values, respectively (Figure 7.5B top panel).

In the immunocompetent C57Bl mice, the decrease in the number of unmodified (i.e. HLA-ABC⁺) hMSCs was more rapid, i.e. on average only about 10% of the input cells remained at two weeks after transplantation (Figure 7.5B middle panel). This difference in the rate of reduction in β -gal activity between the two mouse strains is considered to reflect immune rejection of the hMSCs. Interestingly, following implantation in immunocompetent recipients the US11-hMSCs disappeared faster than the unmodified hMSCs (Figure 7.5B middle panel).

Immunohistological analysis of pinnae at 3, 7 and 14 days after implantation of unmodified hMSCs or US11-hMSCs revealed little cell infiltration at day 3 but massive infiltration of granulocytes and NK cells at day 7, regardless of the MHC class I surface levels of the implanted cells (Figure 7.6). At day 14 after transplantation, only few granulocytes and NK cells were detected in the pinnae (Figure 7.6A, 7.6B and 7.6D). The number of infiltrating CD8⁺ cells was, at all time points significantly higher in pinnae implanted with unmodified hMSCs than in those injected with US11-hMSCs (Figure 7.6D)

To visualize NK cells, consecutive tissue sections were stained with either anti-NKp46, anti-Ly49G2 or anti-NK1.1 antibodies. Although NK1.1⁺CD3⁻ and NK1.1⁺CD3⁺ cells were identified by flow cytometry among peripheral blood mononuclear cells (PBMCs) of C57Bl mice (Figure 7.7), we could not detect NK1.1⁺ cells in sections of pinnae or control tissues (spleen and lymph nodes, data not shown). Accordingly, in Fig. 6 sections stained with the NKp46-specific antibody are presented. Similar frequencies and distributions of positive cells were found in the sections stained with the anti-Ly49G2 antibody (no statistical significant difference, data not shown). Ly49G2 is present on the surface of both NK and NK T cells, in contrast to the NKp46 protein, whose surface expression is essentially restricted to NK cells. Our finding may thus indicate the absence of substantial numbers of NK T cells in the vicinity of the grafted cells.

The knowledge that lack of classical MHC class I surface molecules can render cells susceptible to NK cell-mediated lysis⁴², and the evident infiltration of NK cells into the implantation site, led to the proposition that NK cells are involvement in the early rejection of US11-hMSCs in C57Bl mice.

Indeed, C57Bl recipient mice depleted of NK cells through repeatedly administration of NK1.1-specific antibodies (Figure 7.7) maintained US11-hMSCs implants at levels similar to those in NOD/SCID mice, which naturally display low NK cell activity (Fig. 5B, lower panel). NK cell depletion did not significantly affect the rate of decline of unmodified hMSCs in C57Bl mice. The

difference in the rejection kinetics of US11-hMSCs between C57Bl mice with and without NK cells signifies that US11-hMSCs can trigger NK cell activation *in vivo* and serve as targets for their cytolytic activity.

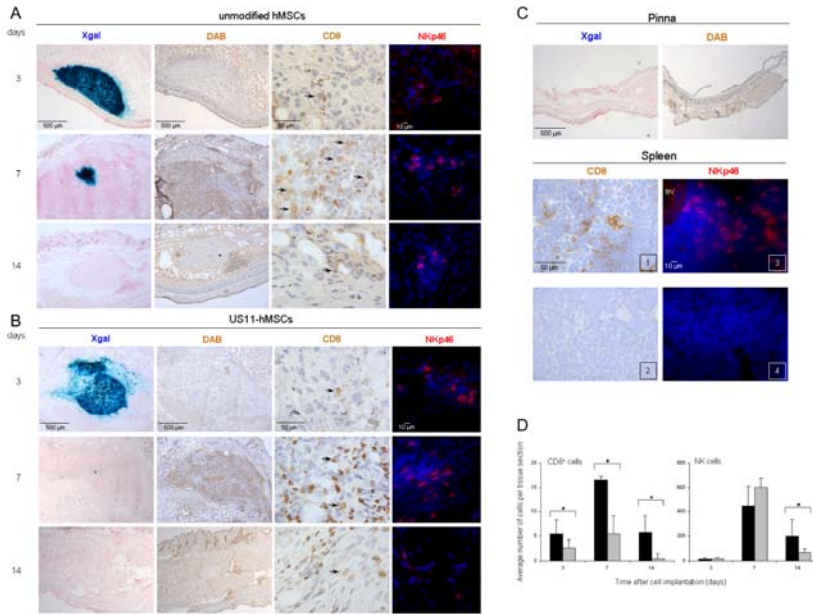


Figure 7.6 Infiltration of recipient's immune cells in the vicinity of the hMSC-implants. Immunohistological and histochemical analysis of frozen tissue section. **(A and B)** Pinnae excised 3, 7 and 14 days after implantation of *LacZ*-transduced hMSCs **(A)** or *LacZ*-transduced US11-hMSCs **(B)**. Implanted hMSCs are visualized in the pinnae by X-gal (blue) staining. DAB staining was used to identify granulocytes (endogenous peroxidase) and CD8⁺ cells. The granulocytes are recognized by the intracellular localization of the brown precipitate while the CD8⁺ cells (arrows) are predominantly showing staining of the plasma membrane. The anti-NKp46 antibody was used to identify NK cells (red, cell membrane staining) and nuclei were stained with Hoechst 33342 (blue). **(C)** Control tissues (pinna and spleen). **(D)** CD8⁺ and NK cell counts in pinnae transplanted with untreated hMSCs (black bars) or US11-hMSCs (gray bars). The data represent averages \pm SD of CD8⁺ and NKp46⁺ cells present in 9 different tissue sections (3 pinnae per experimental group and 3 sections with a mutual distance of 32 μ m per pinna). * $p < 0.05$.

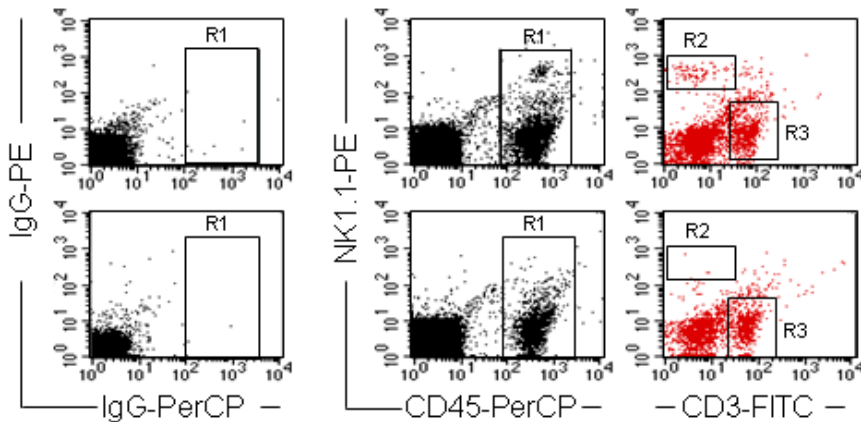


Figure 7.7 **NK cell levels in C57Bl mice treated with NK1.1-specific MAb.** Flow cytometric analysis of PBMCs of a representative mouse stained with antibodies directed to murine CD45, CD3 and NK1.1. The upper panels show data of peripheral blood taken before treatment with NK1.1-specific MAb. The lower panels are derived from a peripheral blood sample taken 7 days after intraperitoneal injection of 100 µg anti-NK1.1 antibodies. Cells stained with isotype-matched control antibodies are depicted in the left column. In the right column only CD45⁺ cells that were gated in R1 (middle column) have been analyzed for surface expression of NK1.1 (gate R2) and CD3 (gate R3). All peripheral blood samples of mice treated with NK1.1-specific MAb showed similar low levels of NK1.1⁺ CD3⁻ cells.

Discussion

Modulation of immunogenicity using viral immune evasion strategies has become a field of active research over the past decade. *In vitro* studies conducted primarily with establish cell lines revealed efficient inhibition of MHC class I/II surface expression after transduction with viral vectors encoding EBV immunoevasins. We show here that of four different herpesviral immunoevasins previously reported to interfere with the MHC class I antigen-presenting pathway, only the HCMV US11 protein strongly downregulates MHC class I expression on the surface of culture-expanded primary hMSCs. The HCMV US2 protein, which like the US11 protein, dislocates class I heavy chain molecules into the cytosol for subsequent degradation by proteasomes³⁹, was less effective in the hMSCs. Using adenoviral vectors, Rehm et al.⁴³ found that in primary human dendritic cells surface MHC class I expression was also suppressed much more efficiently by the US11 protein as compared to the US2 protein while in the human astrocytoma cell line U373 MG both immunoevasins were highly effective. Comparison of the amounts of the US11 and US2 proteins in the two cell types made the authors conclude that the differential

effects of these two immunoevasins on the dendritic cells are not caused by the differences in their steady-state levels. Rather, studies with U373 MG cells expressing different murine class I heavy chain proteins⁴⁴ and J26 cells (i.e. human *B2M*-transduced murine fibroblasts) expressing distinct human HLA-ABC allomorphs^{45,46} revealed that US2- and US11-mediated down-regulation of MHC class I surface expression in these cell types is haplotype-specific. Notably, in our study, hMSCs derived from BM of four donors showed a very similar US2- and US11-dependent decrease in MHC class I surface expression.

The observed differences in the extent to which US2 and US11 inhibit expression of HLA-ABC on the surface of hMSCs may relate to the fact that these immunoevasins depend on distinct cellular proteins for their activity, which may be differently regulated in hMSCs. For example, US11-mediated degradation of MHC class I molecules requires Derlin-1 while the activity of US2 is Derlin-1-independent⁴⁷⁻⁴⁸. Also, ubiquitination of MHC class I heavy chains is essential for their dislocation into the cytosol by US2 but not by US11⁴⁹.

Whatever the underlying cause, the observed difference between distinct herpesviral immune evasion proteins in their capacity to suppress MHC class I expression on the surface of hMSCs argues for the screening of different immunoevasins for each specific target cell type, donor and application.

The utility of a herpesviral immunoevasin to inhibit hMSC rejection has been demonstrated here in a xenotransplantation model. Our results show that permanent interference with surface expression of MHC class I molecules with the aid of the US11 protein facilitates maintenance of the grafted cells in NK cell-depleted immunocompetent mice at levels similar to those obtained in immunodeficient recipients. The rapid decrease of the β -gal activity in the ears of immunocompetent mice following intrapinnal transplantation of *LacZ*-transduced US11-hMSCs, and its prevention by NK cell depletion points to NK cell-mediated rejection of the MHC class I donor cells in this animal model.

The kinetics of donor cell infiltration into the implanted pinna, as observed in this study (Figure 7.6), differs from the acute (within 24 hours) infiltration of innate immune cells into solid organ implants or into sites of cutaneous inflammation⁵⁰⁻⁵¹. We propose that this delay (few cells at day 3 post implantation and high numbers at day 7) is caused by the implanted hMSCs and in particular their ability to modulate the cytokine milieu near the site of cell injection. Implantation of hMSCs into ischemic kidneys resulted, after 24 hours, in an increase in anti-inflammatory cytokine (i.e IL-10) gene expression and in a decrease in mRNA levels for the pro-inflammatory cytokines IFN- γ , TNF- α and IL-1 β ⁵². Interestingly, in MSC-treated infarcted rat hearts pro/anti-inflammatory cytokine gene expression ratios increased between 24 hours and

2 weeks after MSC implantation⁵³. This phenomenon may well explain the delayed leukocyte infiltration following hMSC implantation in our experiments. The elimination of MHC class I⁺ hMSCs by NK cells would be consistent with the “missing self” hypothesis⁵⁴ and the reported prominent role of NK cells in xenograft rejection⁵⁵. Our findings, however, do not concur with other studies reporting engraftment of MHC class I⁺ cells in xenogeneic or allogeneic recipients without active suppression of NK cell activity^{28-32,56}. In view of the different strategies used in these studies (i.e. antibody-mediated masking, *B2M* gene knockout, long-term culture, proteins encoded by the adenoviral early region 3) it is tempting to speculate that the observed differences result from qualitative and quantitative differences in residual HLA antigen expression on the surface of the donor cells. Also the donor cell type and the specific NK cell repertoire of the recipients may have affected the outcome of the experiments. It is worth noting that hMSCs do not persist at constant high levels in immunodeficient mice. A time-related decline in the number of implanted hMSCs, as observed in this study, has also been documented in other xenograft models that enabled quantification of the implanted cells⁵⁷⁻⁵⁹. This disappearance of xenografted cells in the absence of adaptive immune responses is poorly understood. Involvement of host innate immune cells has been proposed but, so far, not proven conclusively^{58,60}. Alternatively, the observed decline may reflect an intrinsic property of implanted “free cells” that have been deposited in an unfavorable microenvironment. This perception is supported by results of Eliopoulos and colleagues, showing a limited persistence of murine MSCs following subcutaneous implantation into syngeneic recipients. Long-term survival of the implanted cells was significantly improved by embedding the MSCs into a matrix prior to implantation, emphasizing that the subcutis represents a suboptimal milieu for MSC transplantation^{27,61}. The observation that US11-hMSC numbers diminish in NK cell-depleted C57Bl mice with similar kinetics as in NOD/SCID mice suggests that *in vivo* these MHC-class I⁺ cells do not activate any other immune effector cells than the NK cells. This is especially interesting in view of our finding that like in *US11*-transduced tumor cell lines⁶², *in vitro* exposure of US11-hMSCs to IFN- γ alleviates the effect of the immunoevasin and upregulates cell surface MHC class II protein expression. Apparently, such upregulation does not occur to any significant extent *in vivo*. Rather, a strong inhibition of the expression of genes encoding pro-inflammatory cytokines including IFN- γ was recorded in injured kidney tissue of rats following administration of MSCs⁵². If the interpretation of our results is correct, endowing hMSCs with the US11 protein and an immunoevasin that efficiently blocks NK cell-mediated cytolysis would result in completely non-immunogenic hMSCs for universal application. Protection against the adverse effects of NK cells could be provided by viruses as well. Human and murine cytomegalovirus, for example, encode MHC class

I-like molecules that can serve as decoys for NK cells^{63,64}. Other strategies to inhibit NK cell-mediated donor cell destruction including interference with their activation receptors and modulation of certain cytokine-dependent signaling pathways have also been described⁶⁵.

In conclusion, we have demonstrated the potency of an HCMV immunoevasin to completely downregulate MHC class I expression on the surface of culture-expanded primary hMSCs. Following subcutaneous implantation into immunocompetent mice, the MHC class I⁺ hMSCs underwent fast rejection that was attributed to NK cell activity. However, in immunocompetent mice depleted of NK cells, US11-hMSCs gradually disappeared at a rate similar to that in immunodeficient hosts. Admittedly it is by no means certain that the xenograft model used in this study is fully predictable for the human situation, but our results show at least the expediency of viral immunoevasins in hMSCs and provide a rationale for transferring additional immunoevasin genes to generate universal donor cells.

References

1. Pittenger MF, Mackay AM, Beck SC, Jaiswal RK, Douglas R, Mosca JD, Moorman MA, Simonetti DW, Craig S, Marshak DR. Multilineage potential of adult human mesenchymal stem cells. *Science* 1999;284:143–147.
2. Smith JR, Pochampally R, Pery A, Hsu SC, Prockop DJ. Isolation of a highly clonogenic and multipotential subfraction of adult stem cells from bone marrow stroma. *Stem Cells* 2004;22:823-831.
3. Knaän-Shanzer S, van de Watering MJ, van der Velde I, Gonçalves MA, Valerio D, de Vries AA. Endowing human adenovirus serotype 5 vectors with fiber domains of species B greatly enhances gene transfer into human mesenchymal stem cells. *Stem Cells* 2005;23:1598-1607.
4. Morandi F, Raffaghello L, Bianchi G, Meloni F, Salis A, Millo E, Ferrone S, Barnaba V, Pistoia V. Immunogenicity of human mesenchymal stem cells in HLA-class I-restricted T-cell responses against viral or tumor-associated antigens. *Stem Cells* 2008;26:1275-1287.
5. Le Blanc K, Tammik C, Rosendahl K, Zetterberg E, Ringden O. HLA expression and immunologic properties of differentiated and undifferentiated mesenchymal stem cells. *Exp Hematol* 2003;31:890-896.
6. Romieu-Mourez R, François M, Boivin MN, Stagg J, Galipeau J. Regulation of MHC class II expression and antigen processing in murine and human mesenchymal stromal cells by IFN- γ , TGF- β , and cell density. *J Immunol* 2007;179:1549-1558.
7. Bartholomew A, Sturgeon C, Siatskas M, Ferrer K, McIntosh K, Patil S, Hardy W, Devine S, Ucker D, Deans R, Moseley A, Hoffman R. Mesenchymal stem cells suppress lymphocyte proliferation in vitro and prolong skin graft survival in vivo. *Exp Hematol* 2002;30:42-48.
8. Di Nicola M, Carlo-Stella C, Magni M, Milanese M, Longoni PD, Matteucci P, Grisanti S, Gianni AM. Human bone marrow stromal cells suppress T-lymphocyte proliferation induced by cellular or nonspecific mitogenic stimuli. *Blood* 2002;99:3838-3843.
9. Corcione A, Benvenuto F, Ferretti E, Giunti D, Cappiello V et al. (2006) Human mesenchymal stem cells modulate B-cell functions. *Blood* 107: 367-372.
10. Rasmusson I, Le Blanc K, Sundberg B, Ringdén O. Mesenchymal stem cells stimulate antibody secretion in human B cells. *Scand J Immunol* 2007;65:336-343.
11. Jiang XX, Zhang Y, Liu B, Zhang SX, Wu Y, Yu XD, Mao N. Human mesenchymal stem cells inhibit differentiation and function of monocyte-derived dendritic cells. *Blood* 2005;105:4120-4126.
12. Ramasamy R, Fazekasova H, Lam EW, Soeiro I, Lombardi G, Dazzi F. Mesenchymal stem cells inhibit dendritic cell differentiation and function by preventing entry into the cell cycle. *Transplantation* 2007;83:71-76.
13. Sotiropoulou PA, Perez SA, Gritzapis AD, Baxevasis CN, Papamichail M. Interactions between human mesenchymal stem cells and natural killer cells. *Stem Cells* 2006;24:74-85.
14. Spaggiari GM, Capobianco A, Becchetti S, Mingari MC, Moretta L. Mesenchymal stem cell-natural killer cell interactions: evidence that activated NK cells are capable of killing MSCs, whereas MSCs can inhibit IL-2-induced NK-cell proliferation. *Blood* 2006;107:1484-1490.
15. Zhang J, Li Y, Chen J, Cui Y, Lu M, Elias SB, Mitchell JB, Hammill L, Vanguri P, Chopp M. Human bone marrow stromal cell treatment improves neurological functional recovery in EAE mice. *Exp Neurol* 2005;195:16-26.
16. Le Blanc K, Rasmusson I, Sundberg B, Götherström C, Hassan M, Uzunel M, Ringdén O. Treatment of severe acute graft-versus-host disease with third party haploidentical mesenchymal stem cells. *Lancet* 2004;363:1439-1441.
17. Ringdén O, Uzunel M, Rasmusson I, Remberger M, Sundberg B, Lönnies H, Marschall HU, Dlugosz A, Szakos A, Hassan Z, Omazic B, Aschan J, Barkholt L, Le Blanc K. Mesenchymal stem cells for treatment of therapy-resistant graft-versus-host disease. *Transplantation* 2006;81:1390-1397.

18. Le Blanc K, Frassoni F, Ball L, Locatelli F, Roelofs H, Lewis I, Lanino E, Sundberg B, Bernardo ME, Remberger M, Dini G, Egeler RM, Bacigalupo A, Fibbe W, Ringdén O; Developmental Committee of the European Group for Blood and Marrow Transplantation. Mesenchymal stem cells for treatment of steroid-resistant, severe, acute graft-versus-host disease: a phase II study. *Lancet* 2008;371:1579-1586.
19. Uccelli A, Moretta L, Pistoia V. Mesenchymal stem cells in health and disease. *Nat Rev Immunol* 2008;8:726-736.
20. Chopp M, Zhang XH, Li Y, Wang L, Chen J, Lu D, Lu M, Rosenblum M. Spinal cord injury in rat: treatment with bone marrow stromal cell transplantation. *Neuroreport* 2000;11:3001-3005.
21. Coyne TM, Marcus AJ, Woodbury D, Black IB. Marrow stromal cells transplanted to the adult brain are rejected by an inflammatory response and transfer donor labels to host neurons and glia. *Stem Cells* 2006;24:2483-2492.
22. Wang Y, Chen X, Armstrong MA, Li G. Survival of bone marrow-derived mesenchymal stem cells in a xenotransplantation model. *J Orthop Res* 2007;25:926-932.
23. Kotobuki N, Katsube Y, Katou Y, Tadokoro M, Hirose M, Ohgushi H. In vivo survival and osteogenic differentiation of allogeneic rat bone marrow mesenchymal stem cells (MSCs). *Cell Transplant* 2008;17:705-712.
24. Prigozhina TB, Khitrin S, Elkin G, Eizik O, Morecki S, Slavin S. Mesenchymal stromal cells lose their immunosuppressive potential after allotransplantation. *Exp Hematol* 2008;36:1370-1376.
25. Zangi L, Margalit R, Reich-Zeliger S, Bachar-Lustig E, Beilhack A, Negrin R, Reisner Y. Direct imaging of immune rejection and memory induction by allogeneic mesenchymal stromal cells. *Stem Cells* 2009;27:2865-2874.
26. Daga A, Muraglia A, Quarto R, Cancedda R, Corte G. Enhanced engraftment of EPO-transduced human bone marrow stromal cells transplanted in a 3D matrix in non-conditioned NOD/SCID mice. *Gene Ther* 2002;9:915-921.
27. Eliopoulos N, Stagg J, Lejeune L, Pommey S, Galipeau J. Allogeneic marrow stromal cells are immune rejected by MHC class I- and class II-mismatched recipient mice. *Blood* 2005;106:4057-4065.
28. Faustman D, Coe C. Prevention of xenograft rejection by masking donor HLA class I antigens. *Science* 1991;252:1700-1702.
29. Pakzaban P, Deacon TW, Burns LH, Dinsmore J, Isacson O. A novel mode of immunoprotection of neural xenotransplants: masking of donor major histocompatibility complex class I enhances transplant survival in the central nervous system. *Neuroscience* 1995;65:983-996.
30. Duan WM, Westerman M, Flores T, Low WC. Survival of intrastriatal xenografts of ventral mesencephalic dopamine neurons from MHC-deficient mice to adult rats. *Exp Neurol* 2001;167:108-117.
31. Rodriguez AM, Pisani D, Dechesne CA, Turc-Carel C, Kurzenne JY, Wdziekonski B, Villageois A, Bagnis C, Breittmayer JP, Groux H, Ailhaud G, Dani C. Transplantation of a multipotent cell population from human adipose tissue induces dystrophin expression in the immunocompetent mdx mouse. *J Exp Med* 2005;201:1397-1405.
32. Zdoroveac A, Doebis C, Laube H, Brösel S, Schmitt-Knosalla I, Volk HD, Seifert M. Modulation of graft arteriosclerosis in a rat carotid transplantation model. *J Surg Res* 2008;145:161-169.
33. Vossen MT, Westerhout EM, Söderberg-Nauclér C, Wiertz EJ. Viral immune evasion: a masterpiece of evolution. *Immunogenetics* 2002;54:527-542.
34. Hansen TH, Bouvier M. MHC class I antigen presentation: learning from viral evasion strategies. *Nat Rev Immunol* 2009;9:503-513.
35. Koppers-Lalic D, Reits EA, Resing ME, Lipinska AD, Abele R, Koch J, Marcondes Rezende M, Admiraal P, van Leeuwen D, Bienkowska-Szewczyk K, Mettenleiter TC, Rijsewijk FA, Tampé R, Neefjes J, Wiertz EJ. Varicelloviruses avoid T cell recognition by UL49.5-mediated inactivation of the transporter associated with antigen processing. *Proc Natl Acad Sci U S A* 2005;102:5144-5149.

36. Hislop AD, Rensing ME, van Leeuwen D, Pudney VA, Horst D, Koppers-Lalic D, Croft NP, Neeffes JJ, Rickinson AB, Wiertz EJ. A CD8+ T cell immune evasion protein specific to Epstein-Barr virus and its close relatives in Old World primates. *J Exp Med* 2007;204:1863-1873.
37. Koppers-Lalic D, Verweij MC, Lipińska AD, Wang Y, Quinten E, Reits EA, Koch J, Loch S, Marcondes Rezende M, Daus F, Bieńkowska-Szewczyk K, Osterrieder N, Mettenleiter TC, Heemskerk MH, Tampé R, Neeffes JJ, Chowdhury SI, Rensing ME, Rijsewijk FA, Wiertz EJ. Varicellovirus UL 49.5 proteins differentially affect the function of the transporter associated with antigen processing, TAP. *PLoS Pathog* 2008;4:e1000080.
38. Wiertz EJ, Jones TR, Sun L, Bogoy M, Geuze HJ, Ploegh HL. The human cytomegalovirus US11 gene product dislocates MHC class I heavy chains from the endoplasmic reticulum to the cytosol. *Cell* 1996;84:769-779.
39. Wiertz EJ, Tortorella D, Bogoy M, Yu J, Mothes W, Jones TR, Rapoport TA, Ploegh HL. Sec61-mediated transfer of a membrane protein from the endoplasmic reticulum to the proteasome for destruction. *Nature* 1996;384:432-438.
40. Wiertz EJ, Devlin R, Collins HL, Rensing ME. Herpesvirus interference with major histocompatibility complex class II-restricted T-cell activation. *J Virol* 2007;81:4389-4396.
41. Wilkinson GW, Tomasek P, Stanton RJ, Armstrong M, Prod'homme V, Aicheler R, McSharry BP, Rickards CR, Cochrane D, Llewellyn-Lacey S, Wang EC, Griffin CA, Davison AJ. Modulation of natural killer cells by human cytomegalovirus. *J Clin Virol* 2008;41:206-212.
42. Gasser S, Raulet DH. Activation and self-tolerance of natural killer cells. *Immunol Rev* 2006;214:130-142.
43. Rehm A, Engelsberg A, Tortorella D, Körner IJ, Lehmann I, Ploegh HL, Höpken UE. Human cytomegalovirus gene products US2 and US11 differ in their ability to attack major histocompatibility class I heavy chains in dendritic cells. *J Virol* 2002;76:5043-5050.
44. Machold RP, Wiertz EJ, Jones TR, Ploegh HL. The HCMV gene products US11 and US2 differ in their ability to attack allelic forms of murine major histocompatibility complex (MHC) class I heavy chains. *J Exp Med* 1997;185:363-366.
45. Barel MT, Hassink GC, van Voorden S, Wiertz EJ. Human cytomegalovirus-encoded US2 and US11 target unassembled MHC class I heavy chains for degradation. *Mol Immunol* 2006;43:1258-1266.
46. Barel MT, Pizzato N, Le Bouteiller P, Weirtz EJ, Lenfant F. Subtle sequence variation among MHC class I locus products greatly influences sensitivity to HCMV US2- and US11-mediated degradation. *Int Immunol* 2006;18:173-182.
47. Ye Y, Shibata Y, Yun C, Ron D, Rapoport TA. A membrane protein complex mediates retrotranslocation from the ER lumen into the cytosol. *Nature* 2004;429:841-847.
48. Loureiro J, Lilley BN, Spooner E, Noriega V, Tortorella D, Ploegh HL. Signal peptide peptidase is required for dislocation from the endoplasmic reticulum. *Nature* 2006;441:894-897.
49. Hassink GC, Barel MT, Van Voorden SB, Kikkert M, Wiertz EJ. Ubiquitination of MHC class I heavy chains is essential for dislocation by human cytomegalovirus-encoded US2 but not US11. *J Biol Chem* 2006;281:30063-30071.
50. Hsieh CL, Obara H, Ogura Y, Martinez OM, Krams SM (2002) NK cells and transplantation. *Transpl Immunol* 9:111-114.
51. Viswanathan K, Dhabhar FS (2005) Stress-induced enhancement of leukocyte trafficking into sites of surgery or immune activation. *Proc Natl Acad Sci U S A*. 102:5808-5813.
52. Tögel F, Hu Z, Weiss K, Isaac J, Lange C et al. (2005) Administered mesenchymal stem cells protect against ischemic acute renal failure through differentiation-independent mechanisms. *Am J Physiol Renal Physiol* 289: F31-F42.
53. Chen G, Nayan M, Duong M, Asenjo JF, Ge Y et al. (2010) Marrow stromal cells for cell-based therapy: the role of antiinflammatory cytokines in cellular cardiomyoplasty. *Ann Thorac Surg* 90:190-197.
54. Ljunggren HG, Kärre K. In search of the 'missing self': MHC molecules and NK cell recognition. *Immunol Today* 1990;11:237-244.

55. Li S, Waer M, Billiau AD. Xenotransplantation: role of natural immunity. *Transpl Immunol* 2009;21:70-74.
56. Kojaoghlanian T, Joseph A, Follenzi A, Zheng JH, Leiser M, Fleischer N, Horwitz MS, DiLorenzo TP, Goldstein H. Lentivectors encoding immunosuppressive proteins genetically engineer pancreatic beta-cells to correct diabetes in allogeneic mice. *Gene Ther* 2009;16:340-348.
57. Lee K, Majumdar MK, Buyaner D, Hendricks JK, Pittenger MF, Mosca JD. Human mesenchymal stem cells maintain transgene expression during expansion and differentiation. *Mol Ther* 2001;3:857-866.
58. Xia Z, Taylor PR, Locklin RM, Gordon S, Cui Z, Triffitt JT. Innate immune response to human bone marrow fibroblastic cell implantation in CB17 scid/beige mice. *J Cell Biochem* 2006;98:966-980.
59. Compte M, Cuesta AM, Sánchez-Martín D, Alonso-Camino V, Vicario JL, Sanz L, Alvarez-Vallina L. Tumor immunotherapy using gene-modified human mesenchymal stem cells loaded into synthetic extracellular matrix scaffolds. *Stem Cells* 2009;27:753-760.
60. Dewan MZ, Terunuma H, Ahmed S, Ohba K, Takada M, Tanaka Y, Toi M, Yamamoto N. Natural killer cells in breast cancer cell growth and metastasis in SCID mice. *Biomed Pharmacother* 2005;59 Suppl 2:S375-S379.
61. Eliopoulos N, Al-Khaldi A, Crosato M, Lachapelle K, Galipeau J. A neovascularized organoid derived from retrovirally engineered bone marrow stroma leads to prolonged in vivo systemic delivery of erythropoietin in nonmyeloablated, immunocompetent mice. *Gene Ther* 2003;10:478-489.
62. Radosevich TJ, Seregina T, Link CJ. Effective suppression of class I major histocompatibility complex expression by the US11 or ICP47 genes can be limited by cell type or interferon- γ exposure. *Hum Gene Ther* 2003;14:1765-1775.
63. Farrell HE, Vally H, Lynch DM, Fleming P, Shellam GR, Scalzo AA, Davis-Poynter NJ. Inhibition of natural killer cells by a cytomegalovirus MHC class I homologue in vivo. *Nature* 1997;386:510-514.
64. Leong CC, Chapman TL, Bjorkman PJ, Formankova D, Mocarski ES, Phillips JH, Lanier LL. Modulation of natural killer cell cytotoxicity in human cytomegalovirus infection: the role of endogenous class I major histocompatibility complex and a viral class I homolog. *J Exp Med* 1998;187:1681-1687.
65. Orange JS, Fassett MS, Koopman LA, Boyson JE, Strominger JL. Viral evasion of natural killer cells. *Nat Immunol* 2002;3:1006-1012.
66. van Tuyn J, Knaän-Shanzer S, van de Watering MJ, de Graaf M, van der Laarse A, Schlij MJ, van der Wall EE, de Vries AA, Atsma DE. Activation of cardiac and smooth muscle-specific genes in primary human cells after forced expression of human myocardin. *Cardiovasc Res* 2005;67:245-255.
67. Barel MT, Pizzato N, van Leeuwen D, Bouteiller PL, Wiertz EJ, Lenfant F. Amino acid composition of $\alpha 1/\alpha 2$ domains and cytoplasmic tail of MHC class I molecules determine their susceptibility to human cytomegalovirus US11-mediated down-regulation. *Eur J Immunol* 2003;33:1707-1716.
68. Barel MT, Rensing M, Pizzato N, van Leeuwen D, Le Bouteiller P, Lenfant F, Wiertz EJ. Human cytomegalovirus-encoded US2 differentially affects surface expression of MHC class I locus products and targets membrane-bound, but not soluble HLA-G1 for degradation. *J Immunol* 2003;171:6757-6765.
69. Swift S, Lorens J, Achacoso P, Nolan GP. Rapid production of retroviruses for efficient gene delivery to mammalian cells using 293T cell-based systems. *Curr Protoc Immunol* 1999;10:Unit 10.17C.
70. de la Garza-Rodea AS, van der Velde I, Boersma H, Gonçalves MA, van Bekkum DW et al. (2010) Long-term contribution of human bone marrow mesenchymal stromal cells to skeletal muscle regeneration in mice. *Cell Transplant*. In press

71. van Tuyn J, Pijnappels DA, de Vries AA, de Vries I, van der Velde-van Dijke I, Knaän-Shanzer S, van der Laarse A, Schaliij MJ, Atsma DE. Fibroblasts from human postmyocardial infarction scars acquire properties of cardiomyocytes after transduction with a recombinant myocardin gene. *FASEB J* 2007;21:3369-3379.
72. Gonçalves MA, Pau MG, de Vries AA, Valerio D. Generation of a high-capacity hybrid vector: packaging of recombinant adenoassociated virus replicative intermediates in adenovirus capsids overcomes the limited cloning capacity of adenoassociated virus vectors. *Virology* 2001;288:236-246.
73. Horst D, van Leeuwen D, Croft NP, Garstka MA, Hislop AD, Kremmer E, Rickinson AB, Wiertz EJ, Rensing ME. Specific targeting of the EBV lytic phase protein BNLF2a to the transporter associated with antigen processing results in impairment of HLA class I-restricted antigen presentation. *J Immunol* 2009;182:2313-2324.
74. Lipińska AD, Koppers-Lalic D, Rychłowski M, Admiraal P, Rijsewijk FA, Bieńkowska-Szewczyk K, Wiertz EJ. Bovine herpesvirus 1 UL49.5 protein inhibits the transporter associated with antigen processing despite complex formation with glycoprotein M. *J Virol* 2006;80:5822-5832.
75. Knaän-Shanzer S, van der Velde-van Dijke I, van de Watering MJ, de Leeuw PJ, Valerio D, van Bekkum DW, de Vries AA. Phenotypic and functional reversal within the early human hematopoietic compartment. *Stem Cells* 2008;26:3210-3217.
76. Montoliu L, Blendy JA, Cole TJ, Schütz G. Analysis of perinatal gene expression: hormone response elements mediate activation of a lacZ reporter gene in liver of transgenic mice. *Proc Natl Acad Sci U S A*. 1995;92:4244-4248.
77. Jain VK, Magrath IT. A chemiluminescent assay for quantitation of beta-galactosidase in the femtogram range: application to quantitation of beta-galactosidase in lacZ-transfected cells. *Anal Biochem* 1991;199:119-124.
78. Eppens EF, van Mil SW, de Vree JM, Mok KS, Juijn JA, Oude Elferink RP, Berger R, Houwen RH, Klomp LW. FIC1, the protein affected in two forms of hereditary cholestasis, is localized in the cholangiocyte and the canalicular membrane of the hepatocyte. *J Hepatol* 2001;35:436-443.

